Letter

Demonstration of the charging progress of quantum batteries

Xiaojian Huang,[1] Kunkun Wang,[2] Lei Xiao,[1] Lei Gao,[1] Haiqing Lin,[3,1,*] and Peng Xue[1,†]
[1]*Beijing Computational Science Research Center, Beijing 100084, China*
[2]*School of Physics and Optoelectronic Engineering, Anhui University, Hefei 230601, China*
[3]*School of Physics, Zhejiang University, Hangzhou 310030, China*

(Received 22 November 2022; accepted 6 March 2023; published 20 March 2023)

We report an experimental simulation of charging process of an XXZ Heisenberg Hamiltonian-driven quantum battery by using single photons and linear optics. We find entanglement is not always the most important resource to boost charging, while coherence plays a nontrivial role. We construct a two-qubit quantum battery and investigate the performance of quantum batteries and their relationship with the amount of entanglement and coherence that arise during the charging process. Our finding offers insights into the design of more efficient quantum devices and advances our understanding of quantum resources.

DOI: 10.1103/PhysRevA.107.L030201

I. INTRODUCTION

To realize the next technical revolution, growing attention has been turned to quantum technologies. On the one hand, researchers have to consider the effect in the framework of quantum mechanics as the miniaturization technology deepens in more and more fields. On the other hand, quantum effects have potential advantages in application, and many breakthrough technologies constructed in the quantum realm have been achieved in different fields, such as quantum sensing [1–3], quantum communication [4,5], and quantum computing [6–8]. With the ever-increasing demand of human society for new energy storage [9], it is natural to reconsider the thermodynamic concepts such as work and heat in quantum thermodynamics [10,11] and ask what advantage a quantum mechanical version of a battery could bring to us. Therefore, quantum batteries have gradually aroused research interests and become a research hot spot.

Quantum batteries were first proposed in 2013 to study energy storage and transfer in two-level systems [12]. They are regarded as N two-level systems connected together by some specific methods. These works focus on the role played by these quantum resources in the charging and discharging process, such as quantum coherence [13,14], quantum entanglement [15,16], quantum discord [17–19], etc. Quantum entanglement has attracted much attention since its inception [20]. Entanglement has been proven to be an effective quantum resource in numerous model protocols [12,21]. However, its role in quantum batteries has always been an open question. There are previous works in which entanglement is not necessary [22,23], or even harmful to quantum charging [24]. Moreover, most of the previous works concentrate on theoretical and numerical aspects, and an experimental evidence in this area is still lacking.

Our work is a proof-of-principle experiment. Following the theoretical idea in Ref. [25], we prove that quantum entanglement does not play a major role in quantum advantages of quantum batteries, compared with quantum coherence. To illustrate this question, we design a charging scheme, in which entanglement is not generated. We consider an XXZ Heisenberg Hamiltonian-driven quantum battery and its charging is driven by an external time-independent Hamiltonian H, which consists of collective charging and noncollective charging. By varying each parameter of H, we conclude that quantum entanglement is not the resource in charging, while coherence is a better resource according to the charging performance.

II. TWO-CELL QUANTUM BATTERIES

Without loss of generality, we consider the Hamiltonian of the quantum battery is [23]

$$H_0 = \hbar\omega_0 \sum_{n=1}^{2} \sigma_n^z, \tag{1}$$

where $\sigma^x, \sigma^y, \sigma^z$ are 2×2 Pauli matrices, ω_0 is the identical Larmor frequency for each qubit, and $\hbar = \omega_0 = 1$. If we use $|\uparrow\rangle$ and $|\downarrow\rangle$ to represent the excited and ground states of a single spin, respectively, we are able to define the fully charged state of the battery as $|\uparrow\uparrow\rangle$ with energy $2\hbar\omega_0$, and the empty state as $|\downarrow\downarrow\rangle$ with energy $-2\hbar\omega_0$. Obviously, the maximal work that can be extracted ($\mathcal{E}_{\max}$) from the battery is $4\hbar\omega_0$. Our aim is to study the quantitative work extracted from a quantum system, so the charging process is not coupling with the environment, in other words, adiabatic [12,26]. As we focus on the effect of interactions and its nature on performance of the battery, the charging Hamiltonian consists of parallel (H_{ch}) and collective charging (H_{int}) [23], that is,

$$H = H_{\text{ch}} + H_{\text{int}}, \tag{2}$$

*hqlin@zju.edu.cn
†gnep.eux@gmail.com

where

$$H_{\rm ch} = \hbar\Omega \sum_{n=1}^{2} \sigma_n^x. \tag{3}$$

The interaction term

$$H_{\rm int} = J\hbar\left(\sigma_1^x\sigma_2^x + \sigma_1^y\sigma_2^y + \Delta\sigma_1^z\sigma_2^z\right) \tag{4}$$

is an XXZ Heisenberg Hamiltonian, where J determines the two-body interaction and dimensionless parameter Δ characterizes the anisotropic interaction [27]. The charging process can be described by a unitary operator U, namely,

$$U = e^{-iHt}. \tag{5}$$

The performance of quantum batteries is reflected by ergotropy $\mathcal{E}$ [23,28] and instantaneous power P. Here, we consider that the state of the battery ρ is a pure state and during the charging process there is no interaction with environment. Hence the state of the battery ρ and ergotropy $\mathcal{E}$ can be expressed as

$$\rho = U\rho_g U^\dagger, \tag{6}$$

and

$$\mathcal{E} = {\rm Tr}\,(\rho H_0) - {\rm Tr}(\rho_g H_0), \tag{7}$$

where ρ_g is the density matrix of the empty state, the so-called passive state [23,25,29,30]. The instantaneous power $P(t)$ is defined as

$$P(t) = \frac{d\mathcal{E}(t)}{dt}. \tag{8}$$

The charging process corresponds to classical parallel charging when we set $J = 0$, as no quantum resource is produced. The ergotropy $\mathcal{E}$ and the instantaneous power P can be calculated analytically [25],

$$\begin{aligned} \mathcal{E}_\parallel(t) &= \mathcal{E}_{\rm max}\sin^2(\Omega t), \\ P_\parallel(t) &= \frac{d\mathcal{E}_\parallel(t)}{dt} = P_{\rm max}^\parallel \sin(2\Omega t), \end{aligned} \tag{9}$$

where the subscript $\parallel$ indicates the parallel charging process and $P_{\rm max}^\parallel = \mathcal{E}_{\rm max}\Omega$. The battery is first fully charged at $t_{\rm min} = \pi/(2\Omega)$. We study the dynamics of charging in $t \in \mathcal{T}_{\rm min} = [0, t_{\rm min}]$. Time interval $\mathcal{T}_{\rm min}$ is appropriate since the quantum correlation we discuss here will shorten the time needed for the battery to reach the maximal $\mathcal{E}$. Otherwise, such a quantum correlation is not a resource [25,29].

The quantum correlations we discuss here are entanglement and coherence. Entanglement can be well quantified by concurrence Q [31]. Given a pure state written in the reference basis as $|\psi\rangle = \alpha_{\uparrow\uparrow}|\uparrow\uparrow\rangle + \alpha_{\downarrow\uparrow}|\downarrow\uparrow\rangle + \alpha_{\uparrow\downarrow}|\uparrow\downarrow\rangle + \alpha_{\downarrow\downarrow}|\downarrow\downarrow\rangle$, we consider the entanglement given by the Wootters' measure of entanglement of a pair of qubits as

$$Q = 2|\alpha_{\uparrow\uparrow}\alpha_{\downarrow\downarrow} - \alpha_{\downarrow\uparrow}\alpha_{\uparrow\downarrow}|. \tag{10}$$

Coherence of a state ρ is defined as [32,33]

$$C_0(t) = \frac{1}{C_{\rm max}}\sum_{i,j\neq i}|\rho_{ij}(t)|, \tag{11}$$

where ρ_{ij} is the element of ρ. The quantity $C_{\rm max} = 3$ is the maximum coherence of a two-qubit system, corresponding to the state $|\Psi_{C_{\rm max}}\rangle = (1/2)(|\uparrow\rangle + |\downarrow\rangle)(|\uparrow\rangle + |\downarrow\rangle)$. We will analyze the role of entanglement and coherence for the charging process of the battery.

III. EXPERIMENTAL IMPLEMENTATION

We experimentally realize the charging process by using single-photon [34–37] and linear optics [38]. Using two spatial modes and polarizations of single photons, the basis states of the battery are encoded as $|\uparrow\uparrow\rangle = |UH\rangle$, $|\uparrow\downarrow\rangle = |UV\rangle$, $|\downarrow\uparrow\rangle = |DH\rangle$, $|\downarrow\downarrow\rangle = |DV\rangle$, where $|U\rangle$ and $|D\rangle$ denote the upper and lower spatial modes of the photons, respectively, while horizontal and vertical polarizations of the photons are represented by $|H\rangle$ and $|V\rangle$.

The initial state is the ground state $|\downarrow\downarrow\rangle$ of the internal Hamiltonian H_0. The initial state preparation is straightforward. After passing through a polarizing beam splitter (PBS), a half-wave plate (H_1) at 45°, and a beam displacer (BD), the transmitted photons in the lower mode with vertical polarization are prepared in $|DV\rangle$.

In order to demonstrate the charging process U in Eq. (5), we need to decompose U using the cosine-sine decomposition method [39–41], which means that U can be decomposed into three experimentally feasible operations, that is,

$$\begin{aligned} U &= \mathbb{L}\mathbb{S}\mathbb{R}, \quad \mathbb{L} = \left(\begin{array}{c|c} L & 0 \\ \hline 0 & L' \end{array}\right), \quad \mathbb{R} = \left(\begin{array}{c|c} R & 0 \\ \hline 0 & R' \end{array}\right), \\ \mathbb{S} &= \begin{pmatrix} \cos\theta_1 & 0 & \sin\theta_1 & 0 \\ 0 & \cos\theta_2 & 0 & \sin\theta_2 \\ -\sin\theta_1 & 0 & \cos\theta_1 & 0 \\ 0 & -\sin\theta_2 & 0 & \cos\theta_2 \end{pmatrix}, \end{aligned} \tag{12}$$

where $\mathbb{L}$ and $\mathbb{R}$ are two-qubit controlled operations, which can be realized by inserting a sandwich-type set of wave plates (WPs) [42] in the corresponding spatial modes. The spatial modes of photons are control qubits and the polarizations are target qubits. The single qubit rotations on the polarizations L (L') and R (R') are realized by the set of WPs.

Similarly, $\mathbb{S}$ can be further decomposed into

$$\mathbb{S} = TST, \tag{13}$$

where

$$T = \begin{pmatrix} 1 & 0 & 0 & 0 \\ 0 & 0 & -1 & 0 \\ 0 & 1 & 0 & 0 \\ 0 & 0 & 0 & 1 \end{pmatrix}, \tag{14}$$

and

$$S = \left(\begin{array}{c|c} H\left(-\frac{\theta_1}{2}\right) & 0 \\ \hline 0 & H\left(\frac{\theta_2}{2} - \frac{\pi}{2}\right) \end{array}\right). \tag{15}$$

As illustrated in Fig. 1, the SWAP operation T can be realize by two BDs and a set of HWPs at 45° and 0°. The two-qubit controlled operation S can be realized by inserting HWP at $-\theta_1/2$ (H_2) and $\theta_2 - \pi/2$ (H_3) into the upper and lower spatial modes, respectively. The evolved states are reconstructed via a two-qubit quantum state tomography [43]. As shown in Fig. 1, a set of WPs, a BD, and a PBS are used to perform the 16 projective measurements in the various bases $|UH\rangle$, $|UV\rangle$, $\frac{|U\rangle(|H\rangle - i|V\rangle)}{\sqrt{2}}$, $\frac{|U\rangle(|H\rangle + |V\rangle)}{\sqrt{2}}$,

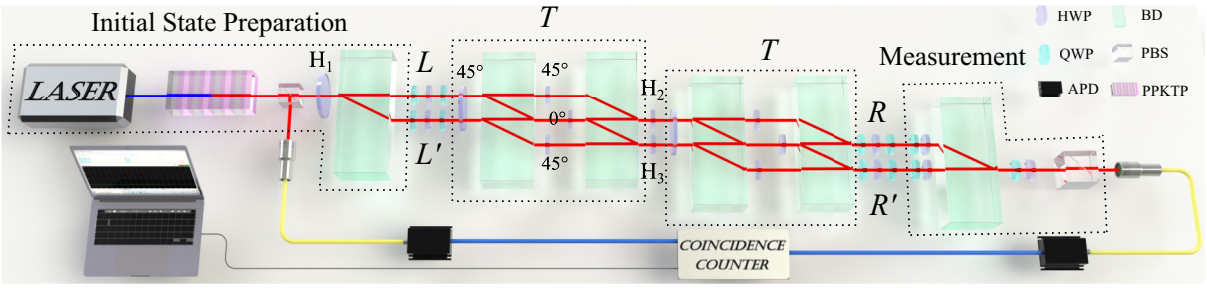

FIG. 1. Experimental setup. By pumping a 20-mm-long type-II periodically poled potassium titanyl phosphate (PPKTP) crystal with a 405-nm continuous-wave diode laser, a pair of photons is generated via the spontaneous parametric down-conversion, with one serving as a trigger and the other as a heralded single photon. The initial state of the two qubits is prepared in $|DV\rangle$ by a single photon undergoing a polarizing beam splitter (PBS), a half-wave plate (HWP), and a beam displacer (BD). Subsequently, a unitary operation is realized on the single photon via an interferometric network consisting of BDs and wave plates (WPs). The unitary operation is decomposed into two-qubit controlled operations (L, R) and two-qubit SWAP operations (T). Two-qubit state tomography is used to measure ergotropy, instantaneous charging power, and the values of entanglement and coherence. Photons are detected by coincidence using silicon avalanche photodiodes (APDs).

$|DH\rangle$, $|DV\rangle$, $\frac{|D\rangle(|H\rangle-i|V\rangle)}{\sqrt{2}}$, $\frac{|D\rangle(|H\rangle+|V\rangle)}{\sqrt{2}}$, $\frac{(|U\rangle-i|D\rangle)|H\rangle}{\sqrt{2}}$, $\frac{(|U\rangle-i|D\rangle)|V\rangle}{\sqrt{2}}$, $\frac{(|U\rangle-i|D\rangle)(|H\rangle-i|V\rangle)}{2}$, $\frac{(|U\rangle-i|D\rangle)(|H\rangle+|V\rangle)}{2}$, $\frac{(|U\rangle+|D\rangle)|H\rangle}{\sqrt{2}}$, $\frac{(|U\rangle+|D\rangle)|V\rangle}{\sqrt{2}}$, $\frac{(|U\rangle+|D\rangle)(|H\rangle-i|V\rangle)}{2}$, $\frac{(|U\rangle+|D\rangle)(|H\rangle+|V\rangle)}{2}$. Photons are detected by coincidence using silicon avalanche photodiodes (APDs). The ergotropy $\mathcal{E}$, instantaneous charging power P, and the values of entanglement Q and coherence C_0 can be calculated by the density matrices of the reconstructed states.

IV. EXPERIMENTAL RESULTS

In order to study the influence of entanglement and coherence on charging process, we choose $\Delta = -1$, $\Delta = 0$, and $\Delta = 1$, and compare the changes of the ergotropy $\mathcal{E}$, the instantaneous charging power P, Q, and C_0 during the charging process. As illustrated in Figs. 2(a) and 2(b), by considering the collective charging progress $J \neq 0$, the ergotropy and the instantaneous power of the quantum battery for different choices of the anisotropy parameter are shown and the experimental results agree well with their theoretical predictions. In Fig. 2(c), one can easily find that concurrence remains nearly zero for $\Delta = 1$, that is, no entanglement is present. However, such zero entanglement production does not mean the battery is classical. The maximum coherence is obtained for $\Delta = 1$ shown in Fig. 2(d). The behavior of the charging progress is enhanced rather than the cases with $\Delta = 0$ and $\Delta = -1$ as $\mathcal{E}$ and P become larger than those for the other two cases. We experimentally verify that entanglement does not benefit the charging progress of the quantum battery and coherence works as a resource to enhance the performance of the quantum battery.

The role of the parameter Δ for the charging process can be better understood by defining the average quantities for charge, power, entanglement, and coherence rather than the instantaneous ones. and neither of can give an unambiguous result alone. In other words, the average quantities $\bar{P}(\Delta)$, $\bar{Q}(\Delta)$, and $\bar{C}(\Delta)$ can be defined in the interval $t \in [0, t_{\min}]$, given by $\bar{X}(\Delta) = (1/t_{\min}) \int_0^{t_{\min}} X(t)dt$. For completeness, we also compute the quantities of ergotropy at the end of the charging $\mathcal{E}_{\text{fin}}(\Delta) = \mathcal{E}(t = t_{\min})$ for various Δ. For our experiment, we choose $\Delta = -1$, -0.75, -0.5, -0.25, 0, 0.25, 0.5, 0.75, 1 and $t = 0$, 0.2, 0.4, 0.6, 0.8, 1. As illustrated in Fig. 3, every data of $\bar{Q}(\Delta)$ and $\bar{C}(\Delta)$ corresponds to the numerical integration of $Q(t)$ and $C(t)$ at the specific Δ by the trapezoidal rule. Experimental results of $\bar{P}(\Delta)$ are integration of lines processed as ones in Fig. 2(b). Obviously, the trends of $\mathcal{E}$ and P along Δ is increasing with a vanishing trend of Q. The averaged entanglement $\bar{Q}(\Delta)$ is zero while $\bar{\mathcal{E}}(\Delta)$ and $\bar{P}(\Delta)$ reach their climax. Quantum advantages here can only be explained by the coherence.

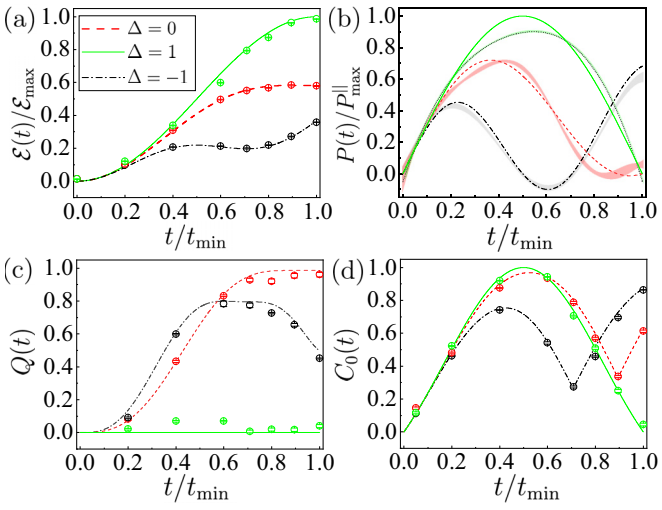

FIG. 2. Experimental results of the time evolution for (a) ergotropy, (b) instantaneous charging power, (c) entanglement, and (d) coherence of the two-cell quantum battery for different values of the anisotropy parameter Δ. We choose $J = \Omega = 0.5\pi$. Theoretical predictions are shown by solid lines, and the corresponding experimental results are shown by symbols. Experimental results represented by the dashed lines in (b) are obtained from the experimental data in (a). With the experimental data in (a) we obtain the function of the ergotropy vs time by numerical fitting, and then derive the instantaneous charging power from the fitting function. The shaded regions are standard deviations of them. Error bars are due to the statistical uncertainty in photon-number counting.

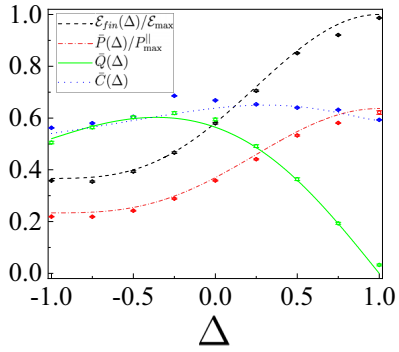

FIG. 3. Experimental results of the quantities $\mathcal{E}_{\text{fin}}(\Delta)$ (in units of $\mathcal{E}_{\max}$), $\bar{P}(\Delta)$ (in units of $P^{||}_{\max}$), $\bar{Q}(\Delta)$, and $\bar{C}(\Delta)$ with $J = \Omega = 0.5\pi$ as a function of Δ. Theoretical predictions are shown by solid lines, and the corresponding experimental results are shown by symbols. Error bars are due to the statistical uncertainty in photon-number counting.

Finally, we study the effect of the coupling strength J, which reveals the relative weight of parallel charging and collective charging. We measure the same quantities introduced in Fig. 2 by setting $\Omega = 1$ and $J = 10^{-1}$, $10^{-0.5}$, 10^{0}, $10^{0.5}$, and 10^{1}. As illustrated in Fig. 4, the average work and power increase and converge to the optimal values given by $\Delta = 1$ with the coupling strength J decreasing. We experimentally witness that the performance of quantum batteries approach to the best by decreasing J as in Figs. 4(a) and 4(b). The best performance is at $\Delta = 1$ regardless of J. Entanglement $\bar{Q}(\Delta)$ still remains zero for $\Delta = 1$. Thus, quantum advantages can only be explained by coherence. Overall, the behavior of $\bar{Q}(\Delta)$ in Fig. 4 has nothing to do with the behavior of $\mathcal{E}_{\text{fin}}(\Delta)$ and $\bar{P}(\Delta)$ when comparing with $\bar{C}(\Delta)$. Our experimental results agree with the theoretical predictions.

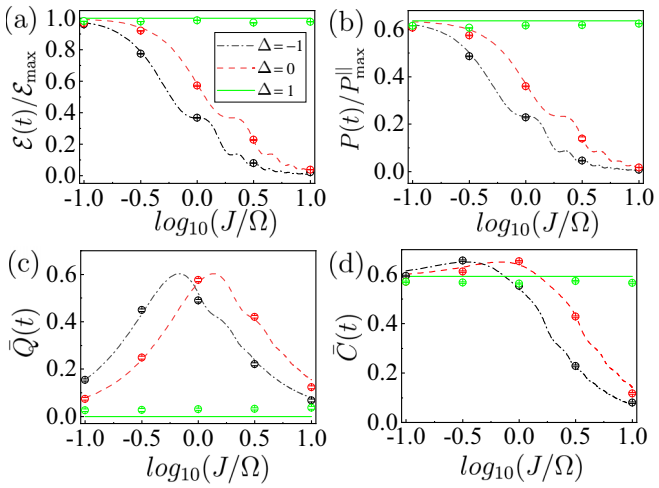

FIG. 4. Experimental results of the quantities $\mathcal{E}$ (in units of $\mathcal{E}_{\max}$), $\bar{P}$ (in units of $P^{||}_{\max}$), $\bar{Q}$, and $\bar{C}$ as a function of J/Ω (in log scale) with various Δ. We choose $\Omega = 0.5\pi$ and $J \in [\frac{\pi}{20}, \frac{\pi}{2\sqrt{10}}, \frac{\pi}{2}, \frac{\sqrt{10}\pi}{2}, 5\pi]$. Theoretical predictions are shown by solid lines, and the corresponding experimental results are shown by symbols. Error bars are due to the statistical uncertainty in photon-number counting.

V. CONCLUSION

In summary, we experimentally demonstrate the charging progress of an XXZ Heisenberg Hamiltonian-driven quantum battery with single photons and linear optics and explore the relation between quantum resources, i.e., entanglement and coherence and the performance of quantum batteries, i.e., ergotropy and instantaneous power. We experimentally study the role of an anisotropy parameter of the XXZ Heisenberg chain Δ and coupling strength J carefully and conclude that entanglement is not the resource that benefits the quantum charging progress. The relation between the amount of entanglement and performance is subtle, and highly relies on the charging system. Our experimental results agree with the theoretical predictions and reveal the nontrivial role of coherence straightforwardly. Our experiment further advances the frontier of quantum batteries and the applications of coherence as a quantum resource.

ACKNOWLEDGMENTS

This work has been supported by the National Natural Science Foundation of China (Grants No. 92265209, No. 12025401, and No. U2230402). H.Q.L. acknowledges support from the National Natural Science Foundation of China (Grant No. 12088101). K.K.W. acknowledges support from the National Natural Science Foundation of China (Grant No. 12104009). L.X. acknowledges support from the National Natural Science Foundation of China (Grant No. 12104036).

APPENDIX: ANALYTICAL EXPRESSIONS OF THE QUANTITIES WHEN $\Delta = 1$

In this Appendix we show how to get the analytical expressions of $\mathcal{E}(t)$, $P(t)$, $Q(t)$, and $C_0(t)$ when $\Delta = 1$. One can easily check that $[H_{\text{ch}}, H_{\text{int}}] = 0$ when $\Delta = 1$. Therefore, Eq. (5) of the main text can be rewritten as $U = e^{-iH_{\text{int}}t}e^{-iH_{\text{ch}}t}$. Given our initial state $|\psi(0)\rangle = |\downarrow\downarrow\rangle = |00\rangle$, where $|\downarrow\rangle$ ($|\uparrow\rangle$) is defined as $|0\rangle$ ($|1\rangle$), one can have, on the basis $\{|\uparrow\uparrow\rangle, |\uparrow\downarrow\rangle, |\downarrow\uparrow\rangle, |\downarrow\downarrow\rangle\}$,

$$|\psi'(t)\rangle = e^{-iH_{\text{ch}}t}|00\rangle = \begin{pmatrix} -\sin^2(\Omega t) \\ -\frac{i}{2}\sin(2\Omega t) \\ -\frac{i}{2}\sin(2\Omega t) \\ \cos^2(\Omega t) \end{pmatrix}. \tag{A1}$$

Then $|\psi(t)\rangle = e^{-iH_{\text{int}}t}|\psi'(t)\rangle$. H_{int} reads

$$H_{\text{int}} = \begin{pmatrix} J & 0 & 0 & 0 \\ 0 & -J & 2J & 0 \\ 0 & 2J & -J & 0 \\ 0 & 0 & 0 & J \end{pmatrix}, \tag{A2}$$

and its eigenvalues and corrresponding eigenvectors are

$$\begin{aligned} E_1 &= -3J, \quad v_1 = \frac{1}{\sqrt{2}}(0,-1,1,0)^{\intercal}, \\ E_2 &= J, \quad v_2 = (0,0,0,1)^{\intercal}, \\ E_3 &= J, \quad v_3 = \frac{1}{\sqrt{2}}(0,1,1,0)^{\intercal}, \\ E_4 &= J, \quad v_4 = (1,0,0,0)^{\intercal}. \end{aligned} \tag{A3}$$

Combining Eqs. (A1) and (A3) one can get

$$|\psi(t)\rangle = e^{-iH_{\rm int}t}|\psi'(t)\rangle = e^{-iJt}\begin{pmatrix} -\sin^2(\Omega t) \\ -\frac{i}{2}\sin(2\Omega t) \\ -\frac{i}{2}\sin(2\Omega t) \\ \cos^2(\Omega t) \end{pmatrix}. \tag{A4}$$

By comparing Eqs. (A1) and (A4) one can see that $e^{-iH_{\rm int}t}$ changes nothing but a phase factor, which implies that the average of an observable O, $\langle\psi(t)|O|\psi(t)\rangle$, is irrelevant to J if such observable itself does not contain the parameter J. This explains why quantities investigated in Fig. 4 of the main text do not change with J when $\Delta = 1$. Furthermore, one can consecutively get the analytical expressions of desired physical quantities, shown in the following,

$$\begin{aligned} \mathcal{E}(t)/\mathcal{E}_{\rm max} &= \sin^2(\Omega t), \\ P(t)/P^{\parallel}_{\rm max} &= \sin(2\Omega t), \\ Q(t) &= 0, \\ C_0(t) &= \tfrac{4}{3}|\sin(2\Omega t)|\cos^2(\Omega t). \end{aligned} \tag{A5}$$

One can see that quantities are the same as the ones of the classical parallel charging cases when $\Delta = 1$. Such a revival can be observed in the dynamics of the concerned physical quantities in Fig. 2 of the main text.

[1] S. Zaiser, T. Rendler, I. Jakobi, T. Wolf, S. Y. Lee, S. Wagner, V. Bergholm, T. Schulte-Herbrüggen, P. Neumann, and J. Wrachtrup, Enhancing quantum sensing sensitivity by a quantum memory, Nat. Commun. **7**, 12279 (2016).

[2] J. M. Boss, K. S. Cujia, J. Zopes, and C. L. Degen, Quantum sensing with arbitrary frequency resolution, Science **356**, 837 (2017).

[3] B. Stray, A. Lamb, A. Kaushik, J. Vovrosh, A. Rodgers, J. Winch, F. Hayati, D. Boddice, A. Stabrawa, A. Niggebaum *et al.*, Quantum sensing for gravity cartography, Nature (London) **602**, 590 (2022).

[4] J. Yin, Y. Li, S. Liao, M. Yang, Y. Cao, L. Zhang, J. Ren, W. Q. Cai, W. Y. Liu, S. L. Li *et al.*, Entanglement-based secure quantum cryptography over 1,120 kilometres, Nature (London) **582**, 501 (2020).

[5] W. Z. Liu, Y. Z. Zhang, Y. Z. Zhen, M. H. Li, Y. Liu, J. Fan, F. Xu, Q. Zhang, and J. W. Pan, Toward a Photonic Demonstration of Device-Independent Quantum Key Distribution, Phys. Rev. Lett. **129**, 050502 (2022).

[6] F. Arute, K. Arya, R. Babbush, D. Bacon, J. C. Bardin, R. Barends, R. Biswas, S. Boixo, F. G. S. L. Brandao, D. A. Buell *et al.*, Quantum supremacy using a programmable superconducting processor, Nature (London) **574**, 505 (2019).

[7] H. S. Zhong, H. Wang, Y. H. Deng, M. C. Chen, L. C. Peng, Y. H. Luo, J. Qin, D. Wu, X. Ding, Y. Hu *et al.*, Quantum computational advantage using photons, Science **370**, 1460 (2020).

[8] Z. Chen, K. J. Satzinger, J. Atalaya, A. N. Korotkov, A. Dunsworth, D. Sank, C. Quintana, M. McEwen, R. Barends, S. Hong *et al.*, Exponential suppression of bit or phase errors with cyclic error correction, Nature (London) **595**, 600 (2021).

[9] X. Luo, J. Wang, M. Dooner, and J. Clarke, Overview of current development in electrical energy storage technologies and the application potential in power system operation, Appl. Energy **137**, 511 (2015).

[10] S. Vinjanampathy and J. Anders, Quantum thermodynamics, Contemp. Phys. **57**, 545 (2016).

[11] D. Farina, G. M. Andolina, A. Mari, M. Polini, and V. Giovannetti, Charger-mediated energy transfer for quantum batteries: An open-system approach, Phys. Rev. B **99**, 035421 (2019).

[12] R. Alicki and M. Fannes, Entanglement boost for extractable work from ensembles of quantum batteries, Phys. Rev. E **87**, 042123 (2013).

[13] T. Baumgratz, M. Cramer, and M.-B. Plenio, Quantifying Coherence, Phys. Rev. Lett. **113**, 140401 (2014).

[14] A. Streltsov, G. Adesso, and M. B. Plenio, Colloquium: quantum coherence as a resource, Rev. Mod. Phys. **89**, 041003 (2017).

[15] R. Horodecki, P. Horodecki, M. Horodecki, and K. Horodecki, Quantum entanglement, Rev. Mod. Phys. **81**, 865 (2009).

[16] M. B. Plenio and S. Virmani, An introduction to entanglement theory, in *Quantum Information and Coherence* (Springer, Cham, 2014).

[17] H. Ollivier and W. H. Zurek, Quantum Discord: A Measure of the Quantumness of Correlations, Phys. Rev. Lett. **88**, 017901 (2001).

[18] A. Bera, T. Das, D. Sadhukhan, S. S. Roy, A. Sen(De), and U. Sen, Quantum discord and its allies: a review of recent progress, Rep. Prog. Phys. **81**, 024001 (2018).

[19] C. Cruz, M. F. Anka, M. S. Reis, R. Bachelard, and A. C. Santos, Quantum battery based on quantum discord at room temperature, Quantum Sci. Technol. **7**, 025020 (2022).

[20] D. Home and F. Selleri, Bell's theorem and the EPR paradox, Riv. Nuovo Cimento **14**, 1 (1991).

[21] D. Ferraro, M. Campisi, G. M. Andolina, V. Pellegrini, and M. Polini, High-Power Collective Charging of a Solid-State Quantum Battery, Phys. Rev. Lett. **120**, 117702 (2018).

[22] K. V. Hovhannisyan, M. Perarnau-Llobet, M. Huber, and A. Acín, Entanglement Generation is Not Necessary for Optimal Work Extraction, Phys. Rev. Lett. **111**, 240401 (2013).

[23] M. Alimuddin, T. Guha, and P. Parashar, Structure of passive states and its implication in charging quantum batteries, Phys. Rev. E **102**, 022106 (2020).

[24] J. X. Liu, H. L. Shi, Y. H. Shi, X. H. Wang, and W. L. Yang, Entanglement and work extraction in the central-spin quantum battery, Phys. Rev. B **104**, 245418 (2021).

[25] F. H. Kamin, F. T. Tabesh, S. Salimi, and A. C. Santos, Entanglement, coherence, and charging process of quantum batteries, Phys. Rev. E **102**, 052109 (2020).

[26] S. Ghosh, T. Chanda, and A. Sen De, Enhancement in the performance of a quantum battery by ordered and disordered interactions, Phys. Rev. A **101**, 032115 (2020).

[27] S. J. Gu, H. Q. Lin, and Y. Q. Li, Entanglement, quantum phase transition, and scaling in the XXZ chain, Phys. Rev. A **68**, 042330 (2003).

[28] A. E. Allahverdyan, R. Balian, and T. M. Nieuwenhuizen, Maximal work extraction from finite quantum systems, Europhys. Lett. **67**, 565 (2004).

[29] G. Francica, F.-C. Binder, G. Guarnieri, M.-T. Mitchison, J. Goold, and F. Plastina, Quantum Coherence and Ergotropy, Phys. Rev. Lett. **125**, 180603 (2020).

[30] M. Perarnau-Llobet, K. V. Hovhannisyan, M. Huber, P. Skrzypczyk, J. Tura, and A. Acín, Most energetic passive states, Phys. Rev. E **92**, 042147 (2015).

[31] W. K. Wootters, Entanglement of Formation of an Arbitrary State of Two Qubits, Phys. Rev. Lett. **80**, 2245 (1998).

[32] J. Monsel, M. Fellous-Asiani, B. Huard, and A. Auffèves, The Energetic Cost of Work Extraction, Phys. Rev. Lett. **124**, 130601 (2020).

[33] B. Çakmak, Ergotropy from coherences in an open quantum system, Phys. Rev. E **102**, 042111 (2020).

[34] P. Grangier, G. Roger, and A. Aspect, Experimental evidence for a photon anticorrelation effect on a beam splitter: a new light on single-photon interferences, Europhys. Lett. **1**, 173 (1986).

[35] P. J. Mosley, J. S. Lundeen, B. J. Smith, P. Wasylczyk, A. B. U'Ren, C. Silberhorn, and I. A. Walmsley, Heralded Generation of Ultrafast Single Photons in Pure Quantum States, Phys. Rev. Lett. **100**, 133601 (2008).

[36] P. Xue, R. Zhang, H. Qin, X. Zhan, Z. H. Bian, J. Li, and B. C. Sanders, Experimental Quantum-Walk Revival with a Time-Dependent Coin, Phys. Rev. Lett. **114**, 140502 (2015).

[37] Z. H. Bian, J. Li, H. Qin, X. Zhan, R. Zhang, B. C. Sanders, and P. Xue, Realization of Single-Qubit Positive-Operator-Valued Measurement via a One-Dimensional Photonic Quantum Walk, Phys. Rev. Lett. **114**, 203602 (2015).

[38] E. Knill, R. Laflamme, and G. J. Milburn, A scheme for efficient quantum computation with linear optics, Nature (London) **409**, 46 (2001).

[39] J. A. Izaac, X. Zhan, Z. Bian, K. Wang, J. Li, J. B. Wang, and P. Xue, Centrality measure based on continuous-time quantum walks and experimental realization, Phys. Rev. A **95**, 032318 (2017).

[40] K. K. Wang, Y. Shi, L. Xiao, J. Wang, Y. N. Joglekar, and P. Xue, Experimental realization of continuous-time quantum walks on directed graphs and their application in PageRank, Optica **7**, 1524 (2020).

[41] P. Xue and Y. F. Xiao, Universal Quantum Computation in Decoherence-Free Subspace with Neutral Atoms, Phys. Rev. Lett. **97**, 140501 (2006).

[42] B. N. Simon, C. M. Chandrashekar, and S. Simon, Hamilton's turns as a visual tool kit for designing single-qubit unitary gates, Phys. Rev. A **85**, 022323 (2012).

[43] D. F. V. James, P. G. Kwiat, W. J. Munro, and A. G. White, Measurement of qubits, Phys. Rev. A **64**, 052312 (2001).